Korea-Australia Rheology Journal
Vol. 19, No. 4, December 2007 pp. 227-232

Effect of shear on poly(styrene-*b*-isoprene) copolymer micelles

Joona Bang[1,*] and Timothy P. Lodge[2]
[1]*Department of Chemical and Biological Engineering, Korea University, Seoul 136-701, Republic of Korea*
[2]*Department of Chemical Engineering & Materials Science, and Department of Chemistry, University of Minnesota, Minneapolis, MN 55455-0431*

(Received July 23, 2007; final revision received November 1, 2007)

Abstract

The use of various shearing apparatuses to study the phase behavior of poly(styrene-*b*-isoprene) diblock copolymer micelles is described. A DMTA rheometer was modified so that one can apply oscillatory shear and obtain the scattering pattern along the shear gradient direction. A cone and plate shear cell was designed to access scattering along the shear vorticity direction, and both oscillatory and steady shear can be applied. The most popular way to employ steady shear on relatively low viscosity fluids is to use a Couette cell, because a high shear rate can be readily achieved without disturbing the sample by overflow. In this work, oscillatory shear was used to obtain a single crystal-like scattering pattern, and thereby to examine the mechanism of the thermotropic transition between face-centered cubic (fcc) and body-centered cubic (bcc) lattices. By applying the steady shear, the response of the fcc lattices to various shear rates is discussed.

Keywords : shear cell, oscillatory shear, steady shear, block copolymer micelles, face-centered cubic (fcc), body-centered cubic (bcc)

1. Introduction

Block copolymers often form spherical micelles in a selective solvent. Under appropriate conditions of concentration and temperature, these micelles pack onto cubic lattices. In this case, the ordered symmetry is either close packed (face-centered cubic, fcc or hexagonally close packed, hcp) or body-centered cubic (bcc), depending on the intermicellar potential. For example, micelles with a short corona have a short-ranged, repulsive interaction between micelles and tend to adopt the close-packed fcc structure, similar to hard spheres. For micelles with a long corona, the interaction between micelles becomes longer-ranged, and favors the less dense bcc structure.

The effect of shear on these cubic phases has been extensively studied, as many applications concerning block copolymer solutions are subjected to strong flows. Gast and coworkers investigated SI diblock copolymers in decane with either an fcc or bcc structure using *in situ* small angle neutron scattering (SANS) (McConnell *et al.*, 1995). Various steady shear rates were applied with a Couette cell. For the fcc phase, the polycrystallinity at low shear rate was induced by "defect-mediated" flow. As the shear rate increases, the transition to sliding close-packed layers was observed. The bcc phase was shown to develop a twin structure, with close-packed {110} planes oriented along the shear plane. At high shear rate, melting of the bcc phase was observed. The resulting scattering patterns were also successfully approximated using a model of the scattering pattern developed by Loose and Ackerson (1994). Analogously, the effect of shear on cubic phases formed by aqueous solutions of PEO based copolymers was examined by several groups (Castelletto *et al.*, 2001; Daniel *et al.*, 2000; Daniel *et al.*, 2001; Diat *et al.*, 1996; Eiser *et al.*, 2000a; Eiser *et al.*, 2000b; Hamley *et al.*, 1998a; Hamley *et al.*, 1998b; Hamley *et al.*, 1998c; Hamley *et al.*, 1998d; Molino *et al.*, 1998). Although there is some difference in the details, the overall features were same as those of McConnell *et al.* (1995), as the sliding layer mechanism was also found in these systems.

In this paper, we will describe various shearing apparatuses (three shear cells) and flow types (oscillatory and steady shear), and their use in the study of the phase behavior of block copolymer micelles. By applying oscillatory shear, a single crystal-like scattering pattern could be generated to investigate the transformation mechanism of the thermotropic fcc to bcc transition. The steady shear was used to examine the effect of shear on the cubic phase along two orthogonal directions by employing two shear cells.

2. Experimental

2.1. Materials

*Corresponding author: joona@korea.ac.kr

Approximately symmetric poly(styrene-*b*-isoprene) diblock copolymers, designated SI(8-7) and SI(15-15), with block molecular weights of 8,000 and 7,000 g/mol, and 15,200 and 15,400 g/mol, respectively, were polymerized by living anionic polymerization using standard procedures (Lodge *et al.*, 2002). The polymers were characterized by size exclusion chromatography (SEC) using both refractive index (Wyatt Optilab) and multiangle light scattering detectors (Wyatt Dawn), and by ^{1}H NMR. SEC determined the number average block molecular weights and the polydispersities, M_w/M_n of 1.01 and 1.02 for SI(8-7) and SI(15-15), respectively. ^{1}H NMR was used to determine the block composition and to estimate the mole percent of 4,1-addition of the PI block (94±1%). The block composition, f, was calculated to be 0.49 and 0.47 for SI(8-7) and SI(15-15), respectively. The solvents di-*n*-butyl phthalate (DBP), diethyl phthalate (DEP), dimethyl phthalate (DMP), and squalane (C30) were purchased from Aldrich and purified by vacuum distillation. The polymer solutions were prepared gravimetrically, with the aid of methylene chloride as a cosolvent. The cosolvent was slowly evaporated off under a stream of nitrogen at room temperature until a constant weight was achieved. The polymer volume fraction, ϕ, was calculated assuming additivity of volumes and densities of 1.043, 1.118, 1.160, 0.810, 1.047 and 0.913 g/cm^3 for DBP, DEP, DMP, C30, PS and PI, respectively.

2.2. *In Situ* Small Angle X-ray Scattering (SAXS)

Synchrotron x-ray measurements were performed using two *in situ* shear cells; a DMTA rheometer (Rheometric Scientific) and a modified cone and plate shear cell, which access along shear gradient and vorticity axes, respectively. The details of these instruments have been described previously (Bang and Lodge, 2003; Wang and Lodge, 2002). In the DMTA, the shear plates (12.5 mm × 12.5 mm) were modified with apertures at the center and covered by Kapton films with a thickness of 50 μm. As illustrated in Fig. 1(a), the x-ray beam was allowed to pass through this parallel plate shear sandwich along the gradient direction. A cone-and-plate shear cell was used to access the vorticity direction (Bang and Lodge, 2003; Caputo, 2002; Caputo *et al.*, 2002). The central portion of a traditional cone-and-plate geometry was removed to create annular fixtures with inner and outer radii of 1.5 and 2.5 cm, respectively. A hole was drilled through the fixed lower annular plate, so that the incident x-ray beam passes through the center of the device, then through the sample on the opposite side of the shear cell. The cone angle is 5°, so the shear cell was tilted to an angle of 2.5° in order for the beam to propagate through the cell horizontally (Fig. 1(b)). With this shear cell, we could also apply either oscillatory or steady shear. These two shear apparatuses were installed on the beam line 5ID-D, in the DuPont-Northwestern-Dow (DND-CAT) station at the Advanced Photon Source, Argonne

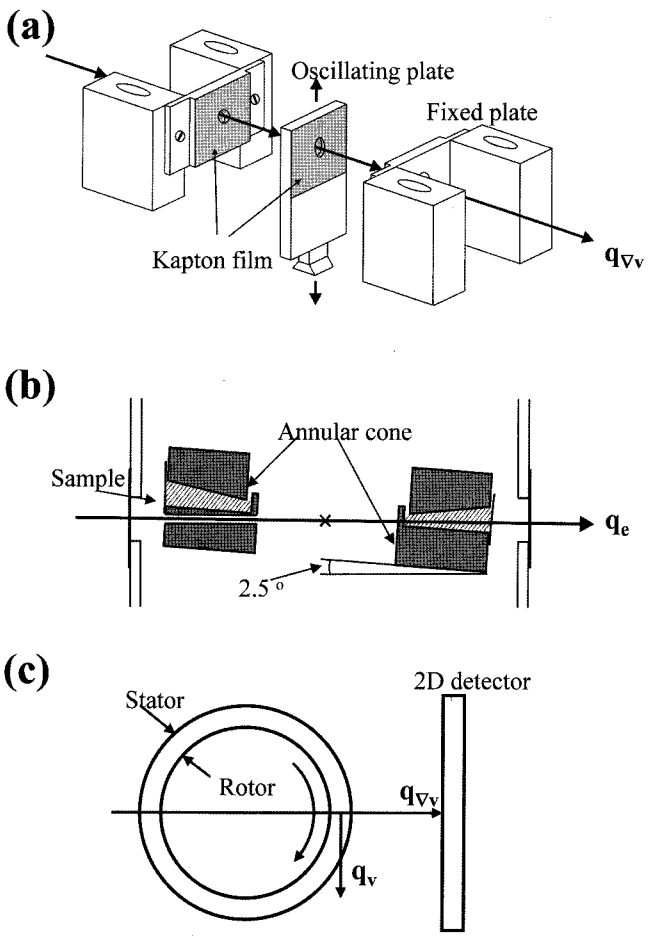

Fig. 1. Schematic illustration of (a) a shear sandwich in the DMTA, (b) a cone and plate shear cell, and (c) a Couette cell.

National Laboratory. 17 keV radiation (λ=0.73 Å) was selected from an undulator beam using a double-crystal monochromator, and then collimated using two sets of adjustable slits. A sample-to-detector distance of 6 m was used to access the necessary q range. 2-D SAXS images were collected using a CCD detector (MAR). For oscillatory shear, the same conditions of strain (γ)=100% and frequency (ω)=1 rad/s were applied for both shear cells.

2.3. Small Angle Neutron Scattering (SANS) with Couette Cell

Neutron scattering experiments were conducted at NIST, Gaithersburg, MD, using the NIST/Exxon/University of Minnesota 30 m SANS instrument (NG7). Neutrons with wavelength λ=6 Å and $\Delta\lambda/\lambda$=0.11 were incident on the sample, and a sample-to-detector distance of 7.0 m was used to yield scattering wave vectors, q, in the range 0.007 Å^{-1}<q<0.098 Å^{-1}. The solution sample, SI(15-15) in C30 with ϕ=0.20, was placed inside a quartz Couette shear cell, and the neutron beam was directed parallel to the shear gradient direction (Fig. 1(c)). A steady shear was produced

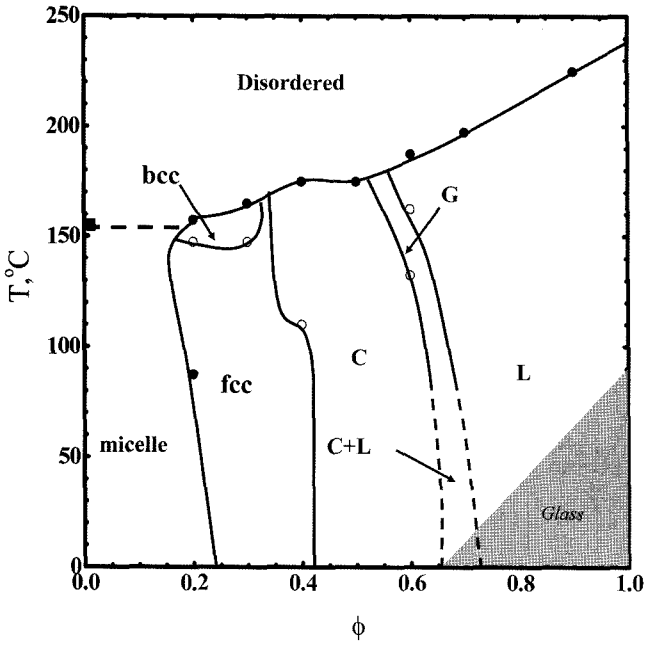

Fig. 2. Phase diagrams for SI(15-15) in DMP as functions of temperature, T, and polymer volume fraction, ϕ. Figure is reproduced from Bang and Lodge (2003).

by rotating the inner rotor, and the shear rates, $\dot{\gamma}$, were accessed in the range of $0.03-400\ s^{-1}$. The solution was heated to 75°C, at which an fcc structure develops (Bang and Lodge, 2004a)., then the various shear rates were applied. At each shear rate, the sample was pre-sheared for 5 – 10 min, and then the data were collected for 10 min with shearing. An interval of at least 15 min between shear rates was allowed. The resulting 2D scattering patterns were collected in an area detector, and the raw data were used without further correction.

3. Results and Discussion

3.1. Thermotropic FCC to BCC transition

We have extensively investigated the phase behavior of SI diblock copolymers in various selective solvents. The detailed phase behavior and a series of phase diagrams have been reported (Hanley *et al.*, 2000; Lodge *et al.*, 2002). Fig. 2 shows an example of a phase diagram for symmetric SI diblock copolymer, SI(15-15), in styrene selective solvent, DMP, and a rich variety of thermotropic and lyotropic phase behaviors can be observed. Among the various OOTs observed, particular interest has been on the thermotropic fcc to bcc transition, and its mechanism and the cause of this transition have been explored recently (Bang and Lodge, 2003; Bang *et al.*, 2002; Bang *et al.*, 2004b; Lodge *et al.*, 2004). To investigate the mechanism of this transition (or any OOT), it would be desirable to obtain the single crystal-like pattern of the parent phase (fcc in our case). Then, the change in the scattering pattern from the parent phase to the newly formed phase (bcc in our case) can be monitored to examine the transformation mechanisms. For this purpose, oscillatory shear has been often applied to produce the single crystal-like patterns.

Previously, the mechanism of the thermotropic fcc to bcc transition was investigated with *in-situ* SAXS. By employing two shear cells, a clear picture of the transformation epitaxy was obtained with the scattering patterns along two orthogonal axes, *i.e.*, the shear gradient and vorticity direction (see Bang *et al.*, 2002 and Bang and Lodge, 2003). Experiments were performed by shearing the solutions in the fcc phase, and then heated to within the temperature window of the bcc phase without shear. In fact, applying oscillatory shear on the fcc solution produced a mixture of fcc and hcp, due to random stacking of the close-packed {111} planes. The corresponding SAXS patterns of fcc/hcp and bcc phases were indexed and the mechanisms and their orientation relationships (ORs) were identified. As a consequence, both the fcc → bcc and hcp → bcc transformations were proposed, and they were described as a modified Bain distortion (Olsen and Jesser, 1971a; 1971b; Shimizu and Nishiyama, 1972; Wada *et al.*, 1989; Wentzcovitch and Krakauer, 1990) and the Burgers mechanism (Bassett and Huang, 1987; Wentzcovitch, 1994; Wentzcovitch and Cohen, 1988), respectively. Both transformations are similar in that the close-packed planes in fcc/hcp ($\{111\}_{fcc}$ and $\{0002\}_{hcp}$ planes) and bcc ({110} planes) remain parallel, and the transformations can be depicted as a relative slippage of the close-packed planes (Wentzcovitch and Krakauer, 1990). Also, there are three degenerate slipping directions, and slipping in one direction results in three orientations of the bcc unit cell by in-plane rotations of 0, $\pm 5.26°$. This gives rise to nine orientations of the bcc unit cell, and they are identical in both transformations. Furthermore, there exist particular ORs between the parent fcc/hcp and the newly formed bcc phase. The ORs of the three bcc unit cells after slipping in one direction correspond to one Nishiyama-Wassermann (N-W) and two Kurdjumov-Sachs (K-S) ORs in the fcc → bcc transformation (Dahmen, 1982; Gotoh and Aral, 1986; Headley and Brooks, 2002). In the case of the hcp → bcc transformation, the analogous ORs to N-W and K-S ORs are referred as Pitsche-Schrader and Burgers ORs, respectively (Dahmen, 1982).

Fig. 3 is an example of SAXS patterns and their peaks assignment for the fcc/hcp and bcc phases along the shear gradient direction. Comparing to Fig. 5 in Bang and Lodge (2003), which was obtained from the lab-source x-ray, a use of the synchrotron produced more higher order reflections in both fcc/hcp and bcc patterns with sharpened peaks; $12\bar{3}0$ and $3\bar{3}00/224$ reflections for fcc/hcp, and 220 and 222 reflections in bcc. All the peaks shown in the bcc phase are significantly smeared azimuthally, and they were indexed as a group of three spots, reflecting three dif-

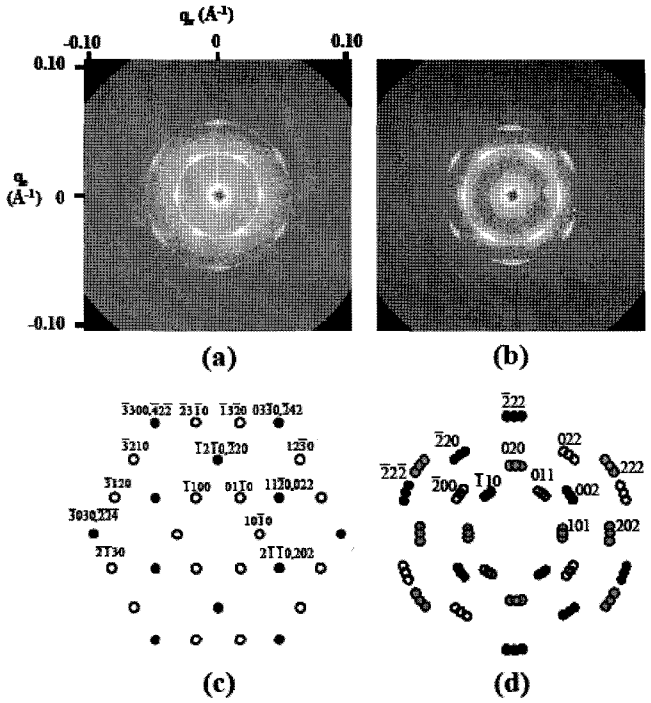

Fig. 3. SAXS patterns for SI(8-7) in DEP $\phi=0.35$ in the shear gradient direction (a) after shearing at 30°C (fcc/hcp) and (b) after heating to 40 °C (bcc) without shear. (c) and (d) represent the indexing of the corresponding SAXS patterns for fcc/hcp and bcc, respectively.

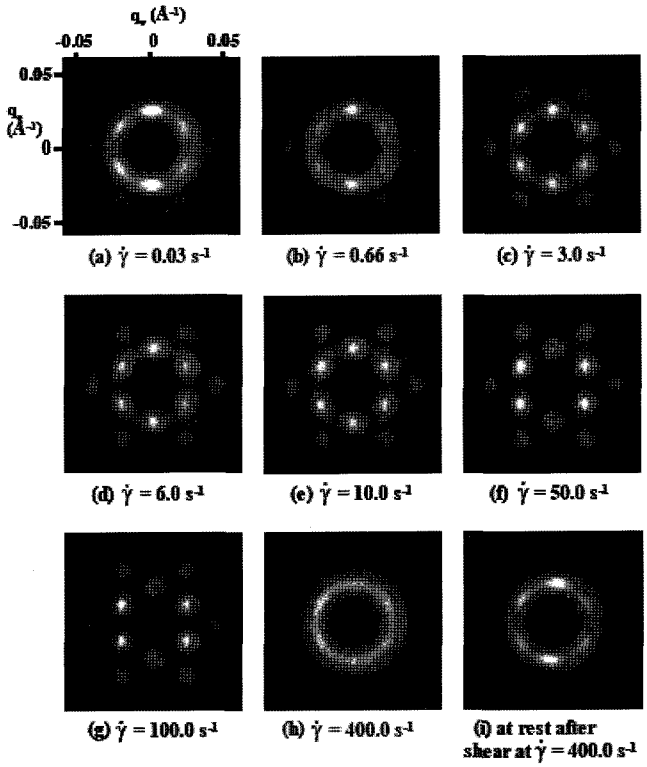

Fig. 4. SANS patterns in the shear gradient direction under various steady shear rate for SI(15-15) in C30 $\phi=0.20$ at 75°C.

ferent orientations of the bcc unit cell after transformations. In this manner, two more reflections were also consistently indexed according to the same mechanisms and ORs we proposed previously, as indicated in Fig. 3(d). For the outermost peaks, *i.e.*, 222 reflections, the appearance of the peaks is different in that the peaks from (222) and $(\bar{2}2\bar{2})$ planes are two times wider than those from $(\bar{2}22)$ plane. This feature was also successfully described such that the wider peaks can be indexed as two adjacent groups of three spots, whereas the peaks from $(\bar{2}22)$ plane are actually a superposition of two groups.

3.2. Effect of Shear on the FCC Phase

The next aspect is the effect of steady shear on the fcc phase. We employed two solutions, SI(15-15) in C30 with $\phi=0.20$, and SI(15-15) in DBP/DEP with $\phi=0.20$. A Couette cell and a cone-and-plate shear cell were used to access the shear gradient and vorticity directions, respectively. The solution of SI(15-15) in C30 with $\phi=0.20$ was investigated using *in situ* SANS. The solution was loaded in a Couette cell at ambient temperature, and then heated to 75°C, where the fcc phase is formed (Bang and Lodge, 2004a). Since the solution consists of a liquid-like, disordered suspension of micelles at ambient temperature, we could completely remove the effect of the alignment caused by inserting rotor. At 75°C, the steady shear was increased incrementally from $\dot{\gamma}=0.03\ s^{-1}$ to $\dot{\gamma}=400.0\ s^{-1}$, as shown by the SANS patterns in Fig. 4. As a complement, SI(15-15) in DBP/DEP with $\phi=0.20$ was examined in the cone-and-plate shear cell using SAXS. Note that this solution forms the fcc lattices at 30°C, at which the shear experiment was performed. Since the viscosity of the solution sample is much lower than the melt, the significant overflow of the sample was observed at high shear rate. Therefore, $\dot{\gamma}$ was limited in the range $0.16\ s^{-1}<\dot{\gamma}<32.0\ s^{-1}$. Fig. 5 displays the corresponding SAXS patterns.

At the shear rates below $1.0\ s^{-1}$, the solution is affected by so-called "defect-mediated" flow (McConnell *et al.*, 1995). In this case, the shear rate is not high enough so that sliding layers-closed packed planes-cannot be easily formed. The resulting scattering patterns have been described as a combination of the powder pattern induced by tumbling crystallites and a small portion of sliding layers. The features in Figs. 4(a) and 4(b) are similar in that the scattering pattern is not well developed, whereas the hexagonal symmetry starts to appear. In addition, it is obvious that the meridional peaks in the first order reflection are much more intense than the other four peaks. This suggests that there is a significant fraction of the closed-packed planes oriented perpendicular to the shear plane, *i.e.*, the velocity (**v**)-vorticity (**e**) plane. In Figs. 5(a) and 5(b) ($\dot{\gamma}<1.0\ s^{-1}$), weak, but clear peaks with hexagonal symmetry are observed in the first and second order reflec-

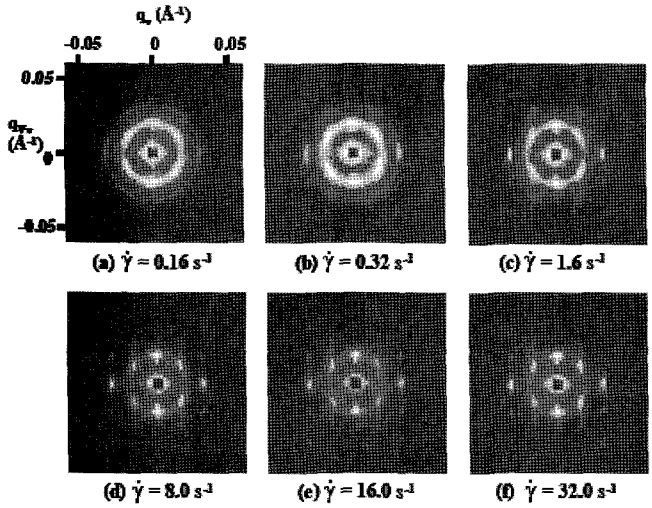

Fig. 5. SAXS patterns in the vorticity direction under various steady shear rate for SI(15-15) in DBP/DEP ϕ=0.20 at 30°C.

tions. This also implies the perpendicular orientations of the closed-packed planes with respect to the shear plane, consistent with Figs. 4(a) and 4(b).

At the intermediate shear rate, $1.0\ s^{-1} < \dot{\gamma} < 50.0\ s^{-1}$, the SANS patterns in Figs 4(c), 4(d) and 4(e) develop the clear peaks with hexagonal symmetry, which is characteristic of an orientation of the closed-packed planes parallel to the shear plane. These patterns were also observed by McConnell *et al.* (Fig. 5.4(d) in McConnell *et al.*, 1995) in this regime. They proposed the layer sliding mechanism as the "slip-stop-slip" motion, such that the layers slip each other by hopping from one registry site to the other, while the resident time for the spheres at one of the registry site is dominant. In other words, the sliding layers can be developed in this regime and overall morphologies in the solution are dominated by the alignment of sliding layers. The SAXS patterns in Figs 5(c), 5(d), 5(e) and 5(f) at this regime are essentially same, and they are characteristic of closed-packed spheres viewed along the vorticity direction. This may also support the mechanism by "slip-stop-slip" motion.

As the shear rate is increased further ($\dot{\gamma} > 50.0\ s^{-1}$), the intensity of two meridional peaks in the first order reflection and two equatorial peaks in the second order reflection diminishes (Figs 4(f) and 4(g)). On the other hand, the intensity of the peaks along two innermost columns increases. This is consistent with a layer sliding mechanism whereby the sliding layers slip past each other rather than hopping to the hollow sites, as presented by Loose and Ackerson (1994). Therefore, the correlation of adjacent closed packed planes becomes weaker due to the higher shear rate. The scattering patterns in this regime are also consistent with McConnell *et al.* (Figs 5.4(e) and 5.4(f) in McConnell *et al.*, 1995).

When the shear rate reaches $\dot{\gamma} = 400.0\ s^{-1}$, the fcc phase is disrupted into the disordered phase, as illustrated in Fig. 4(h). Once the shear was stopped, we observed that the long-range order was recovered (Fig. 4(i)). Therefore, it suggests that the disordered micelles are a metastable phase induced by the strong shear field. Also, note that McConnell and coworkers also observed the loss of long-range order in the bcc phase, but not in the fcc phase (McConnell *et al.*, 1995).

4. Conclusion

In this paper, we described the use of shearing apparatus to investigate transformation mechanisms or to examine the effect of shear in cubic block copolymer micellar phases. By applying the oscillatory shear at the moderate condition ($\gamma = 100\%$ and $\omega = 1$ rad/s), a single crystal-like pattern of fcc phase was obtained. This pattern was then slowly heated to the region of the bcc phase, and the change in the scattering patterns were analyzed according to the transformation mechanism that was established previously (Bang *et al.*, 2002; Bang and Lodge, 2003). The effect of steady shear on the fcc phase was examined along two orthogonal axes. At low shear rate ($\dot{\gamma} < 1.0\ s^{-1}$), the scattering patterns are dominated by "defect-mediated" flow, suggesting that an appreciable fraction of the closed-packed planes are oriented perpendicular to the shear plane. As the shear rate is increased ($1.0\ s^{-1} < \dot{\gamma} < 50.0\ s^{-1}$), the hexagonal symmetry pattern with equally intense spots develops, reflecting the layer sliding mechanism by "slip-stop-slip" motion, as suggested by McConnell and coworkers (McConnell *et al.*, 1995). At higher shear rate ($\dot{\gamma} > 50.0\ s^{-1}$), the scattering patterns imply the layer sliding mechanism without hopping. Eventually, the fcc phase melted away at $\dot{\gamma} = 400.0\ s^{-1}$, leading to the metastable micellar liquids induced by strong shear flow.

Acknowledgements

This work was supported by a Korea University Grant (K0616581), and by the MRSEC Program of the National Science Foundation under Award Number DMR-0212302. Portions of this work were performed at the DuPont-Northwestern-Dow Collaborative Access Team (DND-CAT) Synchrotron Research Center located at Sector 5 of the Advanced Photon Source. DND-CAT is supported by the E.I. DuPont de Nemours & Co., The Dow Chemical Company, the U.S. National Science Foundation through Grant DMR-9304725 and the State of Illinois through the Department of Commerce and the Board of Higher Education Grant IBHE HECA NWU 96. Use of the Advanced Photon Source was supported by the U.S. Department of Energy, Office of Science, Office of Basic Energy Sciences, under Contract No. W-31-109-Eng-38. We thank Dr. Wesley R. Burghardt for making available the cone and

plate shear cell. Further support for this research was provided by the National Institute of Standards and Technology, U.S. Department of Commerce, through the neutron research facilities.

References

Bang, J. and T. P. Lodge, 2003, Mechanisms and epitaxial relationships between close-packed and bcc lattices in block copolymer solutions, *J. Phys. Chem. B* **107**, 12071-12081.

Bang, J. and T. P. Lodge, 2004a, Long-Lived Metastable bcc Phase during Ordering of Micelles, *Phys. Rev. Lett.* **93**, 245701/1-245701/4.

Bang, J., T. P. Lodge, X. Wang, K. L. Brinker, and W. R. Burghardt, 2002, Thermoreversible, epitaxial fcc. to bcc. transitions in block copolymer solutions, *Phys. Rev. Lett.* **89**, 215505/1-215505/4.

Bang, J., K. Viswanathan, T. P. Lodge, M. J. Park, and K. Char, 2004b, Temperature-dependent micellar structures in poly(styrene-b-isoprene) diblock copolymer solutions near the critical micelle temperature, *J. Chem. Phys.* **121**, 11489-11500.

Bassett, W. A. and E. Huang, 1987, Mechanism of the body-centered cubic-hexagonal close-packed phase transition in iron, *Science* **238**, 780.

Caputo, F. E., PhD thesis, Northwestern University, 2002.

Caputo, F. E., W. R. Burghardt, K. Krishnan, F. S. Bates, and T. P. Lodge, 2002, Time-resolved SAXS measurements of a polymer bicontinuous microemulsion structure factor under shear, *Phys. Rev. E* **66**, 041401.

Castelletto, V., I. W. Hamley, P. Holmqvist, C. Rekatas, C. Booth, and J. G. Grossmann, 2001, Small-angle X-ray scattering study of a poly(oxyphenylethylene)-poly(oxyethylene) diblock copolymer gel under shear flow, *Colloid Polym. Sci.* **279**, 621.

Dahmen, U., 1982, Orientation relationships in precipitation systems, *Acta Metall.* **30**, 63.

Daniel, C., I. W. Hamley, W. Mingvanish, and C. Booth, 2000, Effect of shear on the face-centered cubic phase in a diblock copolymer gel, *Macromolecules* **33**, 2163.

Daniel, C., I. W. Hamley, M. Wilhelm, and W. Mingvanish, 2001, Non-linear rheology of a face-centered cubic phase in a diblock copolymer gel, *Rheol. Acta* **40**, 39.

Diat, O., G. Porte, and J.-F. Berret, 1996, Orientation and twins separation in a micellar cubic crystal under oscillating shear, *Phys. Rev. B* **54**, 869.

Eiser, E., F. Molino, G. Porte, and O. Diat, 2000a, Nonhomogeneous textures and banded flow in a soft cubic phase under shear, *Phys. Rev. B* **61**, 6759.

Eiser, E., F. Molino, G. Porte, and X. Pithon, 2000b, Flow in micellar cubic crystals, *Rheol. Acta* **39**, 201.

Gotoh, Y. and I. Aral, 1986, Calculation of interfacial energy of the fcc-bcc interface and its epitaxial orientation relationship, *Jpn. J. Appl. Phys.* **25**, L583.

Hamley, I. W., K. Mortensen, G. E. Yu, and C. Booth, 1998a, Mesoscopic crystallography: a small-angle neutron scattering study of the body-centered cubic micellar structure formed in a block copolymer gel, *Macromolecules* **31**, 6958-6963.

Hamley, I. W., J. A. Pople, C. Booth, L. Derici, M. Imperor-Clerc, and P. Davidson, 1998b, Shear-induced orientation of the body-centered-cubic phase in a diblock copolymer gel, *Phys. Rev. E* **58**, 7620-7628.

Hamley, I. W., J. A. Pople, J. P. A. Fairclough, A. J. Ryan, C. Booth, and Y. W. Yang, 1998c, Shear-induced orientational transitions in the body-centered cubic phase of a diblock copolymer gel, *Macromolecules* **31**, 3906-3911.

Hamley, I. W., J. A. Pople, J. P. A. Fairclough, N. J. Terrill, A. J. Ryan, C. Booth, G.-E. Yu, O. Diat, K. Almdal, K. Mortensen, and M. Vigild, 1998d, Effect of shear on cibic phases in gels of a diblock copolymer, *J. Chem. Phys.* **108**, 6929.

Hanley, K. J., T. P. Lodge, and C.-I. Huang, 2000, Phase behavior of a block copolymer in solvents of varying selectivity, *Macromolecules* **33**, 5918.

Headley, T. J. and J. A. Brooks, 2002, A new bcc-fcc orientations relationship observed between ferrite and austenite in solidification structures of steels, *Metall. Mater. Trans. A* **33A**, 5.

Lodge, T. P., J. Bang, M. J. Park, and K. Char, 2004, Origin of the thermoreversible fcc-bcc transition in block copolymer solutions, *Phys. Rev. Lett.* **92**, 145501.

Lodge, T. P., B. Pudil, and K. J. Hanley, 2002, The full phase behavior for block copolymers in solvents of varying selectivity, *Macromolecules* **33**, 5918.

Loose, W. and B. J. Ackerson, 1994, Model calculations for the analysis of scattering data from layered structures, *J. Chem. Phys.* **101**, 7211.

McConnell, G. A., M. Y. Lin, and A. P. Gast, 1995, Long range order in polymeric micelles under steady shear, *Macromolecules* **28**, 6754.

Molino, F. R., J.-F. Berret, G. Porte, O. Diat, and P. Lindner, 1998, Identification of flow mechnisms for a soft crystal, *Eur. Phys. J.* **B 3**, 59.

Olsen, G. H. and W. A. Jesser, 1971a, The effect of appolied stress on the f.c.c.-b.c.c. transformation in thin iron films, *Acta Metall.* **19**, 1299.

Olsen, G. H. and W. A. Jesser, 1971b, The f.c.c.-b.c.c. transformation in iron deposits on copper, *Acta Metall.* **19**, 1009.

Shimizu, K. and Z. Nishiyama, 1972, Electron microscopic studies of martensitic transformations in iron alloys and steels, *Metall. Trans.* **3**, 1055.

Wada, M., S. Uda, and M. Kato, 1989, The f.c.c. to b.c.c. transformation in Fe film on a spherical Cu substrate, *Phil. Mag. A* **59**, 31.

Wang, C.-Y. and T. P. Lodge, 2002, Kinetics and mechanisms for the cylinder-to-gyroid transition in a block copolymer solution, *Macromolecules* **35**, 6997.

Wentzcovitch, R. M., 1994, hcp-to-bcc pressure-induced transition in Mg simulated by ab initio molecualr dynamics, *Phys. Rev. B* **50**, 10358.

Wentzcovitch, R. M. and M. L. Cohen, 1988, Theoretical model for the hcp-bcc transition in Mg, *Phys. Rev. B* **37**, 5571.

Wentzcovitch, R. M. and H. Krakauer, 1990, Martensitic transformation of Ca, *Phys. Rev. B* **42**, 4563.